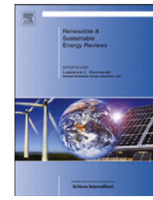
Renewable and Sustainable Energy Reviews 16 (2012) 5355–5362

Contents lists available at SciVerse ScienceDirect

Renewable and Sustainable Energy Reviews

journal homepage: www.elsevier.com/locate/rser



Modeling of phase change materials for applications in whole building simulation

Parham A. Mirzaei, Fariborz Haghighat*

Department of Building, Civil and Environmental Engineering, Concordia University, Montreal, Canada H3G 1M8

ARTICLE INFO

Article history:
Received 29 August 2011
Received in revised form
26 April 2012
Accepted 28 April 2012
Available online 6 July 2012

Keywords:
Thermal storage
Phase change materials
Modeling
Building load calculation
Integrated design

ABSTRACT

The advanced buildings of tomorrow will need to take advantage of renewable, ambient and waste energy to approach ultra-low energy buildings. Such buildings will need to consider Thermal Energy Storage (TES) techniques customized for smaller loads.

Recently, TES has attracted increasing attention due to the potential benefits it can deliver in energy efficiency, shift load from peak to off-peak, economics and environmental impact. Advanced design tools and technical improvements are required in TES technology and systems. Indeed the design of the building and the TES are often not coordinated. A building integrated with distributed thermal storage materials could shift most of peak load to off-peak time period.

Even though various tools have been developed to model the behavior of applied phase change materials (PCM), unacceptable accuracy and/or high computational time are addressed as their major drawbacks. This implies that the development of a fast and reliable model is necessary in order to simulate the long-term behavior of these materials, especially for design and optimization.

Therefore, a new and fast one-dimensional analytical model is proposed in this paper. The PCM behavior is modeled using a RC-circuit concept containing variable capacities for resistant and capacitor. In this approach, the length of mushy, solid, and liquid phases in each period of time signifies the RC capacity. In order to evaluate the performance of the proposed model, a computational fluid dynamics (CFD) model is then developed. The prediction of the newly developed model is compared with the prediction made by the CFD. There are good agreements between the predictions, and the results clearly show the high performance of the proposed model.

Contents

1. Introduction

Building sector contributes immensely to the total energy consumption, particularly for its space conditioning and domestic hot water. In Quebec, 70% of residential buildings use electrical space heating system which accounts for 30% of the grid critical peak, while 91% of domestic water heaters are electric and they account for 1750 MW of the grid peak [1]. At the Canadian level, the domestic water heater accounts for 22% of the total energy use for households. According to Hydro Quebec [2], the marginal cost to supply electricity during the peak period in winter is 10 $/kW and will be increased up to 40 $/kW by 2015. At the same time, in Canada, new buildings are being built at rate of 1% and old buildings stock is retrofitted at the rate of 2.2% annually which

* Corresponding author. Tel.: +1 514 848 2424 93; fax: +1 514 848 7965.
E-mail address: haghi@bcee.concordia.ca (F. Haghighat).

1364-0321/$ - see front matter © 2012 Elsevier Ltd. All rights reserved.
http://dx.doi.org/10.1016/j.rser.2012.04.053

Nomenclature

x	space coordinate (m)
c_P	specific heat (J/kg K)
t	time (s)
T	temperature (K)
K	thermal conductivity (W/mK)
α	thermal diffusivity (m^2/s)
β	liquid fraction
λ	latent heat (kJ/kg)
ρ	density (kg m^{-3})
q	heat flux (W/m^2)
E	released energy (W/m^2)
μ	dynamic viscosity (Pa s)
u	Fluid velocity (m/s)
s	surface position (m)
l	length in one specific time (m)
L	total length (m)
H	total volumetric enthalpy (J)

Subscripts

S	solid
F	fluid
M	mushy
W	wall

Non-dimensional numbers

Re	Reynolds
Nu	Nusselt
Pr	Prandtl

means by 2030 almost 50% of the existing would be retrofitted. Taking this information into account, shifting a significant portion or the whole required energy for space heating and domestic water heating to off-peak periods would have significant economic effects on both energy supply and demand. This shifting technique is accomplished by storing energy during off-peak periods to be utilized during peak periods. Building envelope and central thermal storage have been used as thermal energy storage (TES). Recent study also showed that integration of PCM in building envelope can reduce the urban heat island (UHI) phenomena and improve pedestrian comfort and health [3,4].

Recently, TES has attracted increasing attention due to the potential benefits it can offer in energy efficiency, in shifting load from peak to off-peak, in emergency heating/cooling load, in economics and in environmental impact. Nonetheless, advanced design tools and technical improvements are required in TES technologies and systems. Indeed the design of the building and TES are often not coordinated. A building integrated with distributed thermal storage materials could shift most of peak load to off-peak time period as it is important to plan for the requirements of the buildings of the future. Hence, research is needed to ensure that the actual performance of buildings with TES in use matches expectation and predictions more closely. The use of TES requires smart energy management in buildings to achieve the overall goal of net zero energy buildings. It is desirable to develop technical solutions and tools that incorporate advanced TES material to provide alternative option to conventional solutions and to meet the energy demands of buildings of the future (*SMART NET-ZERO BUILDINGS*).

As part of Annex 23, an international survey was carried out to review the actual implementation of TES use in energy efficient buildings. The results showed that the sensible thermal storage (e.g., water heating system and geothermal) and latent thermal storage (ice) are mature technologies with mostly existing reliable design and system integration tools. The results of the survey also indicated that there is a lack of knowledge and design tools for sizing, optimization, system integration and control of other type of latent thermal storages such as phase change materials (PCM). PCM has been considered as excellent candidate to be used as TES due to its high capacity to store energy. It can be integrated as layer in a wall [5,6], in a floor or ceiling combined by a heating system [7].

Despite many publications, only very limited integration of PCM in existing buildings can be found, and there is almost no information regarding validated design tools for such applications. Most researchers have used in-house solution without any systematic comparison with other alternative design approaches [8]. It is desirable to develop technical solutions and tools that incorporate advanced TES to provide alternative energy option to conventional solutions and to meet the energy demands of future buildings. Also, the existing techniques for so called "passive design" require to be pursued with greater vigor, supported by improved building thermal simulation to optimize their performance. PCM can be embedded within walls and other construction materials to moderate temperature variations and act to enhance thermal capacity as well as to shift load from peak to off-peak. Application of PCM in building construction materials has not been fully exploited and is generally underutilized. Further research has shown that the application of PCM-impregnated gypsum board in a naturally ventilated passive solar building reduced the heating demand up to 90% during autumn and spring [9]. It was concluded that further research is needed to make it efficient for heating season.

The performance of the passive design depends on the function of building, office or residential buildings, and its relation between the PCM type and its position with the building envelope as well as its location within a room in a building. For example, PCM can be either introduced in the insulation, in the interior finishing or in the storage (i.e., hot water tank); further research is needed to optimize the whole system. Numerical analysis of thermal effects of hollow core concrete slabs is well documented. Many simulations have been performed to determine the effects of air flow rate, hollow core diameter and inlet air temperature on the energy saving and thermal load shift properties of hollow core slabs [10]. In addition, PCMs has been incorporated in the construction of hollow core slabs. Moreover, their effects on the slab energy saving in a mild climate have been investigated [11]. The combination of thermal mass and phase change materials shows great promise in terms of energy saving. Efficient simulation tools are needed to investigate the range of parameters and the impact different climate on its performance, and the cost.

Analysis and design of TES for future buildings has to account for several interactions of complex physical processes inherent to this system. Although existing building simulation tools can model building envelopes, thermal mass or duct systems, they cannot efficiently and accurately model double skin façades integrated with TES [12] and/or dynamic insulation walls imbedded with PCM [13]. These tools cannot also accurately model the complex interaction processes between PCM and the building.

Computational Fluid Dynamics (CFD) codes have been widely used in the simulation of PCM. Experimental data have been used for qualitative and/or quantitative validation of the CFD simulations [8]. Though the prediction by these models is generally similar to that of CFD, they are not efficient design tools. Development of a validated

simplified model is a challenging task since modeling PCM involves transient non-linear phenomena with a moving liquid–solid interface whose position is unknown a priori. The existing approaches are not efficient for the design of an energy efficient building integrated with TES. Most of existing PCM models for integration in buildings and even those being implemented in building simulation programs (TRNSYS, EnergyPlus) present some major limitations. As an example, the model developed by Ibánez et al. requires experimental data for the system to be designed, which cannot be readily used for new and innovative designs and optimization [14]. Also, the 3D model developed by Lamberg et al. requires extensive calculation time, which makes its use impractical for design and optimization purposes [15,16]. Dutil et. al carried out a comprehensive review of the existing PCM models and reported that "*many of the recent studies discuss their results qualitatively only as the comparison with a graph taken from publications*…" [8]. Therefore, a new generation of efficient design tools and their comprehensive validation are needed.

This paper reports the development of a simplified model for application of PCM TES in the building simulation programs. It is a fast, efficient and validated model that can be used in the design of an energy efficient building or TES.

2. Brief review on existing models

Stefan problem is attributed to type of problems with changing phase boundary with time. Various analytical solutions in different situation were first introduced by Jozef Stefan [8,17]. These solutions are mostly one-dimensional and defined in semi-infinite or infinite regions. The assigned boundary and initial conditions are also simple and mostly constant while the mushy zone is not considered in solutions.

Numerical techniques have been carried out to model not only the moving boundary of phases, but also to calculate the velocity of mushy region. In one approach, the main assumption is Stefan condition in which latent heat either can be absorbed or desorbed in boundaries:

$$\rho\lambda\frac{ds(t)}{dt}=K_s\frac{\delta T_s}{\delta t}-K_f\frac{\delta T_f}{\delta t} \tag{1}$$

However, it should be noted that discontinuity could occur in numerical model between solid and fluid phases due to a difference in physical properties. As another technique, the behavior of mushy zone can be simulated using enthalpy approach [18]. In this model, conservation of energy can be expressed in terms of total volumetric enthalpy and temperature as bellow:

$$H=\int_{T_{\text{ref}}}^{T}c_P dT+\rho\beta\lambda \tag{2}$$

Here, the first and second parts represent the sensible enthalpy and the latent heat, respectively. Therefore, the energy equation in the PCM can be written as:

$$\frac{\partial}{\partial t}(\rho H)+\nabla.(\rho\vec{u}H)=\nabla.(K\nabla T)+S \tag{3}$$

where S is the source term and different treatments have been proposed to address this term specially in mushy region.

Different techniques (i.e., finite difference, finite element, and finite volume) are also widely used to solve enthalpy-based equations of PCM. Even though the results are mostly acceptable and reliable for a wide range of engineering problems, dealing with above mentioned methods is not always a straight forward procedure, and oscillation of temperature in some occasion is broadly reported [19]. Nonetheless, advanced computational techniques (e.g., using moving meshes or refining meshes within boundary regions) helped to improve the accuracy of these methods. The main drawback of such techniques is still related to their intensive time and CPU cost, where annual simulation is mainly deemed for building energy calculation.

Furthermore, other forms of the continuity and momentum equations are adapted to model the PCM. For example, the temperature transforming model (TTM) keeps velocity at zero [20] or variable viscosity of the medium (VVM) approach sets the viscosity within a high value in the solid phase [21]. Both methods, however, again have difficulties in conserving continuity and code development.

Transfer function is a traditional way to model transient effect in building energy load calculation [22,23]. Recently, a conduction transfer function (CTF) model is adapted for application of the PCM in buildings using response factor to relate the current and past heat flux to current and past temperatures of the building element. This procedure assumes that materials' density, thermal conductivity and specific heat are constant for the period of a simulation where this is not a valid assumption for the PCM, since their phase and properties are continuously changing. Basic formulation of this method presumes a simple relation between heat capacity and temperature. The accuracy of such models is not acceptable although it might be improved assuming various layers for the PCM. Again, shortcoming of this method is addressed for annual thermal load calculations and uncertainty on accuracy improvement. Energy Plus, DOE-2 and BLAST are comprehensive and computationally efficient tools for annual building energy load calculations which are developed based on the CTF method. Barbour and Hittle [24] suggested obtaining a set of CTFs and switching them between the phases. Their results, however, show an error of 20%, which is not acceptable for the design of energy efficient buildings.

Another concept is to model the PCM with one or various set of constant resistant and capacitors (RC) even though assuming one RC circuit cannot provide proper accuracy. On the other hand, more advanced techniques should be integrated to the multiple sets of RCs' model (e.g., genetic algorithm) in order to optimize series of capacitance and resistance [25]. This indicates that intensive efforts are needed for the development of such model for building energy simulation purposes. Moreover, expecting higher accuracies requires increasing the number of RCs, which enormously affect the computational efforts. Table 1 briefly summarizes all existing models for the PCM modeling in term of accuracy and computational time in building applications. Unlike presented models in Table 1, the proposed model in the next section claims to provide an acceptable accuracy and a low computational load.

3. Proposed model

As discussed earlier, RC models are reliable techniques even though their accuracy significantly depends on the number of synchronized RC-circuits. This means that higher number of RC-circuits increases simultaneously their accuracy and CPU time. Therefore, having only one RC-circuit would not satisfy the expected accuracy. In this study, a new one-circuit RC model is developed with a considerable higher accuracy. Unlike the traditional models, the capacity of the capacitor and resistant varies with time in the current model. Depending on existence/

Table 1
Available approaches to model phase change materials in building applications.

Approach	Accuracy	Time and CPU cost
Enthalpy models	Good	Very high
TTM and VVM	Acceptable	Very high
RC models	Fair	High
CTF	Fair	Medium
Stefan models	Poor	Low

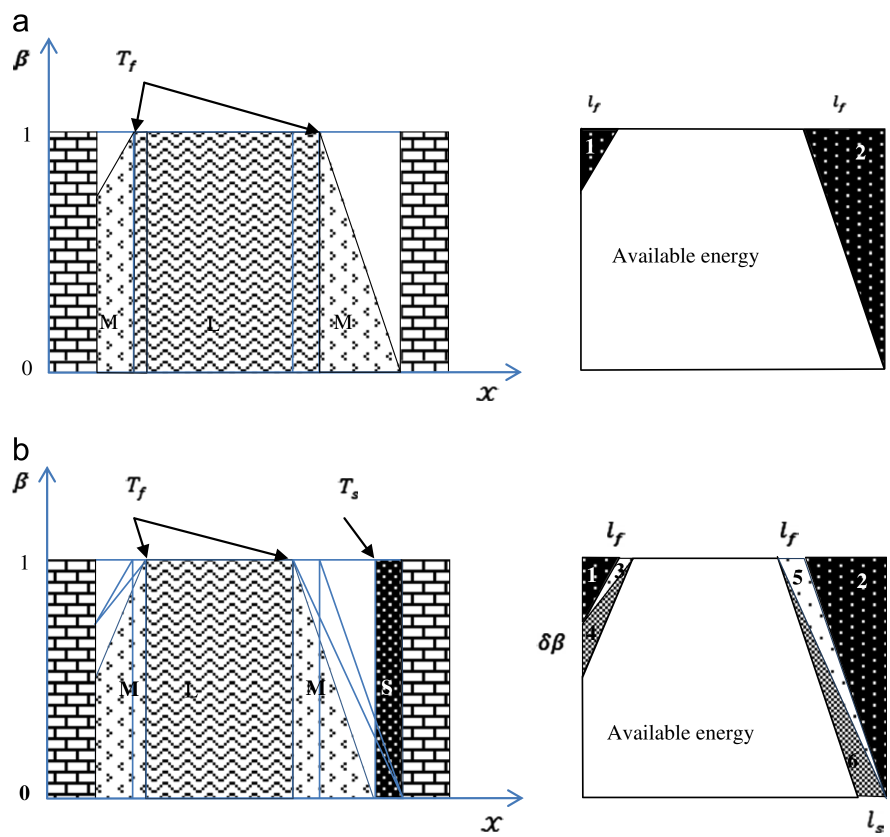


Fig. 1. Reduction of latent heat energy during solidification process. (a) Left wall: S2 and right wall S2mechanisms and (b) Left wall: S1 & S2 and right wall S2 & S3mechanisms.

coexistence of mushy, solid, or liquid phases in each time step, a value can be assigned to a single RC-circuit. For example, when solid phase changes to mushy and liquid phases, the capacity of the RC-circuit alters accordingly. The length of each phase therefore presents the capacity of the RC-circuit during each period of time.

3.1. Solidification process

The proposed model consists of three phases; fluid, mushy, and solid. The temperature of mushy zone is assumed to vary linearly between solidification (T_s) and melting temperatures (T_f) of the PCM. Therefore, the liquid fraction can be defined as below:

$$\beta=(T-T_s)/(T_f-T_s) \tag{4}$$

where in solid phase $\beta=0$ and in fluid phase $\beta=1$

While it is assumed that thermal stratification can be neglected due to the thickness of the PCM, the heat is expected to one-dimensionally conduct through the wall and the PCM. As depicted in Fig. 1, the area under diagram $\beta-x$ shows the potential energy deposited in mushy-phase or liquid-phase of the PCM, and the alteration of this area thus denotes the released energy:

$$\Delta E=\int_{l_1}^{l_2}\rho\lambda\beta dx \tag{5}$$

Illustrated in Fig. 1(a) and (b), the PCM with a greater temperature than T_f has initially a latent energy $E=L_{\mathrm{PCM}}\times\rho\times\lambda(\beta=1)$ During solidification process, the PCM loses part of its energy until it reaches its solidification temperature ($\beta=1$). It should be noted that losing energy could occur either by a decrease in level of liquid fraction or an increase in length of mushy-zone. In general, the conducted heat fluxes through the left and right walls define the form of the energy release/gain, which can be in a combination of the following three mechanisms:

S1-Decrease in level of the liquid fraction in mushy-phase
S2-Conversion of liquid-phase to mushy-phase
S3-Conversion of mushy-phase to solid-phase

Since liquid fraction (β) changes linearly between solid-phase and liquid-phase, the energy release defined in Eq. (5) can be shown by different triangles in Fig. 1. For example, triangles 1 and 2 (Fig. 1a) represent released energy due to change of liquid-phase to mushy-phase (S2), and as depicted in Fig. 1(b), triangles 3 and 5 are again related to alteration of the liquid-phase to mushy-phase. On the other hand, triangle 4 shows how energy is released when level of the liquid fraction is decreased in the mushy-phase (S1). Moreover, triangle 6 displays released energy related to change of the mushy-phase to solid-phase (S3).

The energy release process similar to triangles 5 and 6 (right wall in Fig. 1(b)) is due to phase change of mushy to solid and liquid to mushy. As depicted in Fig. 2, therefore, $E_{mushy\rightarrow solid}$ can be calculated as the area between line 1 and 2 or hatched triangle. Similarly, $E_{liquid\rightarrow mushy}$ is related to the area between line 2 and 3 or shaded triangle (Fig. 2). On the other hand, the length of mushy zone is initially $L_m=l_m+l_s$. This means that the initial profile of the mushy region can be exhibited by line 1. Then, part of the mushy-PCM energy (equal to hatched triangle) is released. Therefore, line 2 depicts a new linear profile of β. The new length of mushy zone is also equal to l_m. Eventually, another portion of liquid-PCM energy (equal to shaded triangle) is released which changes the length of the mushy-PCM to l_m+l_f. Line 3 illustrates the final linear profile of β. Therefore, the whole process implies that the level of mushy-PCM energy is reached from line 1 to line 3. The same analogy can be used to explain the behavior of a process similar to Fig. 1(b) on the left wall where part of the energy release is due to the change of liquid-phase to mushy-phase (triangle 3) and part is due to a decrease in the level of the liquid fraction (triangle 4).

3.2. Melting process

The same analogy can be used to model melting process of the PCM. Conducted heat transfer through walls is accumulated in the PCM in three different forms:

M1-Increase in level of the liquid fraction in mushy-phase
M2-Conversion of mushy-phase to liquid-phase
M3-Conversion of solid-phase to mushy-phase

Obviously, the formation of the above mentioned mechanisms or their combinations depends on heat fluxes in both left and right walls. For example, Fig. 3 demonstrates a situation in which, first, both walls absorb energy through mechanism M3. This implies that triangles 1 and 2 show the amount of energy accumulated in the PCM through mechanism M3. Second, M1 and M3 mechanisms contribute, respectively to deposit energy in the left-side of the PCM where M2 and M3 are attributed to absorb energy in the right-side (Fig. 3(b)). Again, triangles 3 and 6 represent the growth of the mushy region. Triangle 4, however, is related to M1 or the increase in the level of liquid fraction in mushy-phase. Eventually, triangle 5 depicts the absorbed energy due to transformation of the solid-phase to mushy-phase.

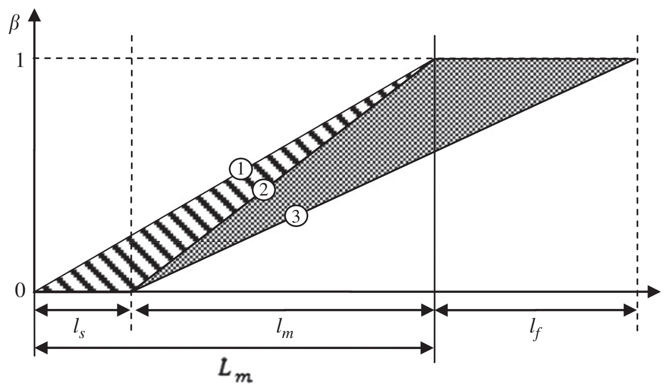


Fig. 2. Energy release with length change of the mushy-PCM.

3.3. Methodology

Modeling of the PCM behavior with variable capacitor concept is explained in this section. First, in the proposed model, each phase is assigned to one node. For example, Fig. 1(a) and (b) can be simulated with two and three nodes, respectively, or Fig. 3(a) and (b) can be presented with two and three nodes since solid-mushy and solid-mushy-liquid phases coexist together, respectively. Then, energy balance can be written for each node assuming variable length for existing phases. The variable lengths are later considered to calculate the capacity of the RC-circuit in each period of time.

For example, using electrical network method, the proposed one-dimensional model for solidification process, when all three phases coexist together, is illustrated in Fig. 4. Presented in Eq. (6), a portion (l_s) of solidified mushy-PCM (q_2) in addition to conducted heat from mushy-zone (q_3) supply conducted heat through the left boundary condition ($q_1 = q_{lb}$). Exhibited in Eq. (7), the conducted heat from mushy-zone (q_3) is simultaneously

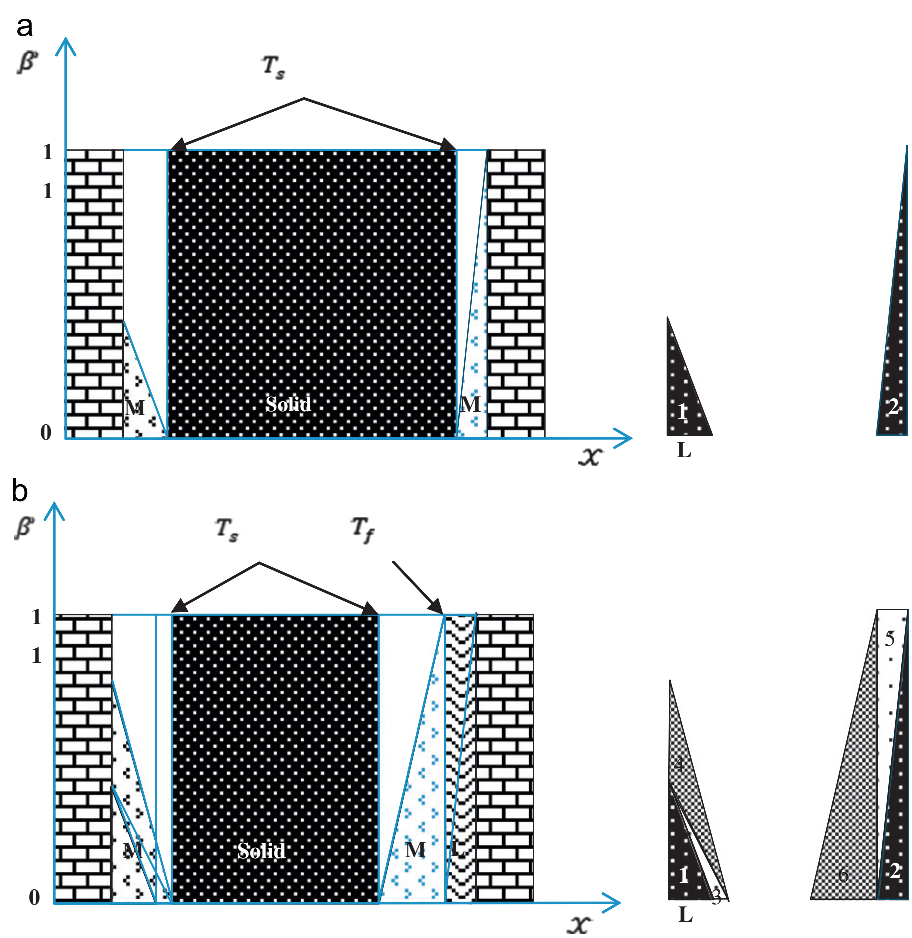


Fig. 3. Accumulation of latent heat energy during melting process. (a) Left wall: M3 and right wall M3 mechanisms @ time t and (b) Left wall: M1 & M3 and right wall M2 & M3 mechanisms @ time t + dt.

provided by alteration of a portion (l_f) of liquid-PCM to mushy-PCM (q_4), and transfer of generated heat (q_6), if the liquid-PCM has higher temperature than T_f, through the mushy zone integrated with coming heat from right boundary condition (q_{rb}). Eventually, conversion of phases' length to each other has to be conserved according to Eq. (9).

$$q_2+q_3=q_1=q_{lb} \Rightarrow \frac{(T_f-T_s)}{\frac{L_m+l_f-l_s}{K_m}}+E_{mushy\to solid}=\frac{(T_s-T_w)}{\frac{L_s+l_s}{K_s}} \quad (6)$$

$$q_5+q_4=q_3 \Rightarrow \frac{T-T_f}{\frac{L_f}{Nu.K_f}}+E_{liquid\to mushy}=\frac{(T_f-T_s)}{\frac{L_m+l_f-l_s}{K_m}} \quad (7)$$

$$q_6+q_{rb}=q_5 \Rightarrow \rho_f c_{pf} L_f \dot{T}+q_{rb}=\frac{T-T_f}{\frac{L_f}{Nu.K_f}} \quad (8)$$

$$L_{PCM}=L_m+L_s+L_f \quad (9)$$

where L_{PCM} is the total length of the PCM and is a constant number. The following empirical equation can be also used to express Nusselt number [26]:

$$Nu=0.664\times Re^{0.5}\times Pr^{0.33} \quad (10)$$

As shown in Eqs. (6) through (10), left and right boundary conditions can be easily assigned to this model in order to find the unknown variables; l_s, l_f, and T. However, to solve these equations, it is necessary to first obtain the released energy from phase changes within the PCM, including $E_{mushy\to solid}$ and $E_{liquid\to mushy}$.

To calculate ΔE presented in Eq. (5), one can assume linear regression for changing density and liquid fraction of the PCM in mushy zone as bellow:

$$\rho_1=\rho_s+\frac{(\rho_f-\rho_s)}{l_s+l_m}x, \quad \beta_1=\frac{x}{l_s+l_m} \quad (11)$$

$$\rho_2=\rho_s+\frac{(\rho_f-\rho_s)}{l_m}(x-l_s), \quad \beta_2=\frac{x-l_s}{l_m} \quad (12)$$

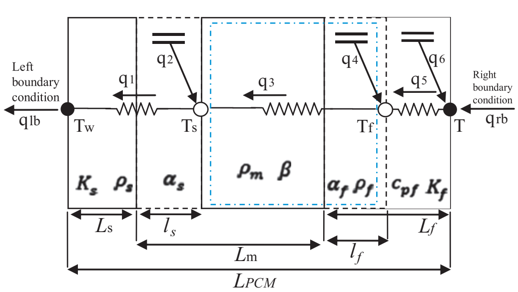


Fig. 4. Schematic of proposed 1-dimensional model.

$$\rho_3=\rho_s+\frac{(\rho_f-\rho_s)}{l_m+l_f}(x-l_s), \quad \beta_3=\frac{x-l_s}{l_m+l_f} \quad (13)$$

Hence, the alteration of energy in mushy-PCM through the hatched and shaded triangles can be obtained from the following equations:

$$q_4=E_{liquid\to mushy}=\frac{\lambda}{\Delta t}\left[\int_{l_s}^{l_s+l_m}(\rho_2\beta_2-\rho_3\beta_3)dx+\int_{l_s+l_m}^{l_s+l_m+l_f}(\rho_f-\rho_3\beta_3)dx\right] \quad (14)$$

$$q_3=E_{mushy\to solid}=\frac{\lambda}{\Delta t}\left[\int_0^{l_s}\rho_1\beta_1 dx+\int_{l_s}^{l_s+l_m}(\rho_1\beta_1-\rho_2\beta_2)dx\right] \quad (15)$$

Again, Eqs. (14) and (15) are developed based on unknown variables of l_m, l_s , and l_f. Thus, Eqs. (5) through (15) can be used to find these variables at each time step with calculation of new L_M, L_s and L_f as below:

$$(L_s)_{new}=(L_s)_{old}+l_s \quad (16)$$

$$(L_f)_{new}=(L_f)_{old}-l_f \quad (17)$$

$$(L_m)_{new}=(L_m)_{old}-l_s+l_f \quad (18)$$

4. Results

The performance of the proposed one-dimensional model is validated with a benchmark (task C) defined by ANNNEX 23 [27]. This task includes several one-dimensional case studies in order to simulate the behavior of a wallboard containing the PCM. In test cases of the task C, the long-wave and short-wave radiations are assumed to be neglected. Moreover, the convective heat transfer coefficients are assigned as two constant values both for left-side and right-side boundary conditions (Table 2). Here, the case study has selected a 10 mm sheet of the PCM without insulation (case study P10). PCM characteristics in addition to initial and boundary condition are also provided in Table 2 (case A). It should be mentioned that the proposed model is indirectly validated with P10 case study as demonstrated in Fig. 5. It means that a two-dimensional computational fluid dynamics (CFD) model based on enthalpy equations is first implemented to model the above mentioned case study. The main reason for carrying out the indirect validation is for comparing the speed of the proposed model with a two-dimensional accurate but time consuming model.

A structured 40×500 mesh domain ($0.01\ m\times0.21\ m$) is generated for two-dimensional CFD domain. The buoyancy effect is not considered in order to convert the problem to a one-dimensional case. Moreover, the conductivity is presented with two

Table 2
PCM characteristics, initial, and boundary conditions.

The PCM characteristic and Boundary Condition	TASK C Case A	Solidification Case B	Melting Case C
Length (m)	0.01	0.01	0.01
Left-side convective heat transfer coefficient (W/m^2K)	2.5	10	5
Right-side convective heat transfer coefficient (W/m^2K)	8.0	10	20
Density ($kg.m^2$)	1100	1100	860
Specific heat (J/kg K)	80,000	140,000	100,000
Conductivity (W/mK)	0.25 ($T<285$)	0.25 ($T<285$)	0.23
	0.20 ($285<T$)	0.20 ($285<T$)	0.23
Solidification temperature (K)	281	287	290
Melting temperature (K)	301	289	299
Left-side air temperature (K)	293	283	300
Right-side air temperature (K)	$285+20t/3600$	283	302
The initial PCM temperature (K)	285	290	285

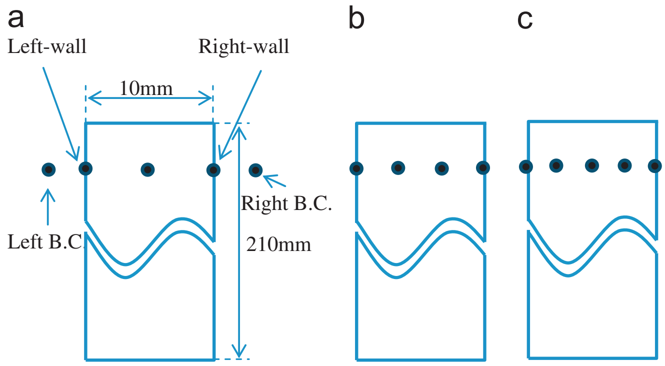


Fig. 5. One dimensional modeling of the PCM sheet (P10) with coexistence of (a) only one phase, (b) two-phases and (c) three-phases.

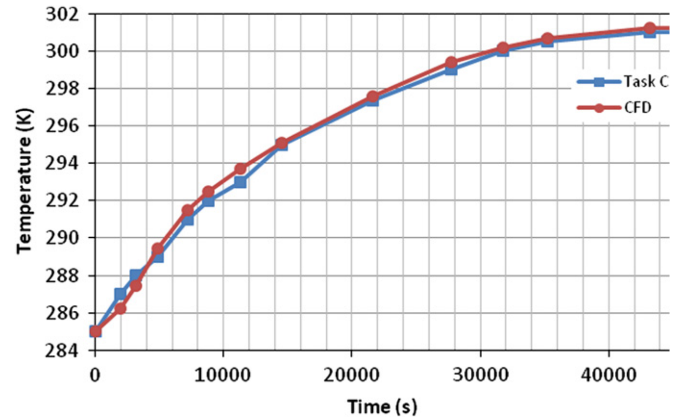


Fig. 6. Comparing obtained results of the CFD model and task C (Case A).

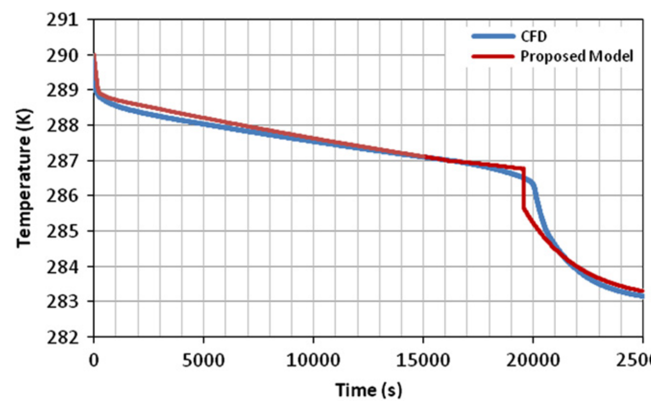


Fig. 7. Comparison of the proposed (Case B) and CFD models for solidification process.

numbers below and above 285 K. Second-order upwind is also considered as discretization scheme for the momentum. Furthermore, a convergence criterion is applied to keep residuals less than 10^{-5} for energy and continuity equations.

A MATLAB code is developed to evaluate the performance of the proposed model. As discussed earlier, the number of nodes represents the coexistence of phases (Fig. 5). When the PCM only contains one phase (pure solid or liquid), one node is used to simulate its behavior. With a same analogy, two or three nodes are employed when two (solid-mushy or liquid-mushy) or three phases (solid-mushy-liquid) coexist together. The distance between nodes is also calculated based on equation given in the previous section. The proposed model automatically switches between one, two, and three nodes depending on the temperature imposed by left and right boundaries. In other words, the length of each phase provides the existence of one, two, or three nodes and the required distance between them.

The validated CFD model is later used for evaluation of the proposed model. For this purpose, two more cases (B and C) are, respectively defined for solidification and melting to show the performance and flexibility of the proposed model.

As illustrated in Fig. 6, the results of CFD model for left-wall temperature show good agreement with corresponding temperature of the above mentioned case study of task C. The average discrepancy of the CFD model from provided results is less than 0.4 K with maximum error of 0.8 K. After validation of the CFD model with the outcomes of Task C, the CFD model itself was applied for evaluation of the proposed model.

Solidification process is simulated with both CFD and proposed models (Case B). As shown in Table 2, the case study B is similarly defined for one layer PCM wall. The characteristic of the PCM and boundary conditions are completely different from the validation case study of task C in order to exhibit the flexibility of the proposed model.

The comparison of two models is depicted in Fig. 7. It can be seen that the proposed model perfectly simulates the temperatures above solidification temperature (T_s=297 K). The mean and maximum errors are, respectively around 0.11 K and 0.60 K during solidification process. When temperature fluctuates between T_f and T_s, the Case B has discrepancy below one percent except for small numbers close to the solidification temperature (T_s). This error is related to the change of entire mushy-phase to solid-phase, which causes a sudden decrease in resistance through the PCM. The trend of the temperatures below T_s and duration of whole process are also successfully simulated with the proposed model (Fig. 7).

Furthermore, the performance of the proposed model to simulate the melting process is examined by introducing a new case study (C) with a new PCM as shown in Table 2. Here, the solidification and melting temperatures are selected to be 290 K and 299 K, respectively. As exhibited in Fig. 8, both CFD and developed models (Case C) present the melting of the PCM in three parts: below T_s, between T_s and T_f, and above T_f.

The proposed model can fairly follow the obtained temperatures in left-wall (Fig. 5) of the CFD model since the turning point in three main parts are almost the same for both models. Both models reach T_s=297 K at the same time, although the Case C reaches T_f around only 400 s prior to the CFD model. The greatest discrepancy is related to the point where the temperature elevates from T_f=299 K. The mean and maximum errors are also calculated as 0.44 K and 1.30 K, respectively.

5. Conclusion

The thermal energy storage must be designed to respond to the actual need of the building. To design a TES that could meet the building of the future requirements, it must be an integral part of the system of the building design. This requires a reliable and fast simulation tool that can be used for design and optimization application.

A new and fast one-dimensional analytical model is proposed for simulating PCM behavior using a RC-circuit concept containing variable capacities for resistant and capacitor. In this method, the length of mushy, solid, and liquid phases in each period of time signifies the RC capacity. In order to evaluate the performance of the proposed model, a CFD model is first developed and validated with a well-defined benchmark [27]; task (C). After successful development of the CFD model, the solidification and melting process of the proposed model are validated under

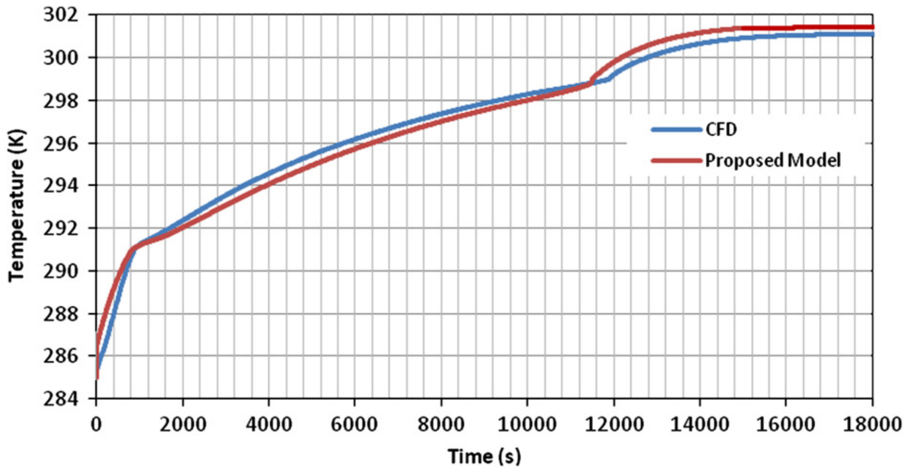


Fig. 8. Comparison of the proposed (Case C) and CFD models for melting process.

various PCM characteristics, boundary, and initial conditions. The obtained results show the considerable capability of the proposed model in order to simulate the behavior of the PCM. The obtained mean errors for solidification and melting process are, respectively 0.11 K and 0.44 K.

There are good agreements between the predictions, and the results clearly show the high performance of the proposed model. Unlike simple RC-circuit models, the advantage of this model is due to its variable resistance and capacity assigned as elements of the PCM. Furthermore, expanding the proposed 1D model to a 2D space would be a ground breaking research topic.

Acknowledgment

The authors would like to express their gratitude to the Public Works and Government Services Canada, and Concordia University for the financial support and Ms. Farinaz Haghighat for his careful reading and corrections.

References

[1] Hydro Quebec. (2007) demande R-3648-2007. Hydro Quebec Distribution -1. Régie de l'énergie du Québec 〈http://www.regie-energie.qc.ca/en/index.html〉.
[2] Hydro Quebec. (2011) Demande R-3776-2011 Hydro Quebec Distribution -2. Régie de l'énergie du Québec 〈http://www.regie-energie.qc.ca/en/index.html〉.
[3] Mirzaei PA, Haghighat F. Approaches to study urban heat island: abilities and limitations. Building and Environment 2010;45(10):2192–201.
[4] Mirzaei PA, Haghighat F. A procedure to quantify the impact of mitigation techniques on the urban ventilation. Building and Environment 2012;47:410–20.
[5] Scalat S, Banu D, Hawes D, Paris J, Haghighat F, Feldman D. Full scale thermal testing of latent heat storage in wallboard. Solar Energy Materials and Solar Cells 1996;44:49–61.
[6] Banu D, Feldman D, Haghighat F, Paris J, Hawes D. Energy Storing Wallboard: Flammability Tests. Journal of Materials in Civil Engineering 1998:98–105.
[7] Koschenz M, Lehmann B. Development of a thermally activated ceiling panel with PCM for application in lightweight and retrofitted buildings. Energy and Buildings 2004;36:567–78.
[8] Dutil Y, Rousse D, Ben Salah N, Lassue S. A review on phase-change materials: mathematical modeling and simulations. Renewable and Sustainable Energy Reviews 2011:31–50.
[9] Heim D, Clarke JA. Numerical modelling and thermal simulation of PCM-gypsum composites with ESP-r. Energy and Buildings 2004;36:795–805.
[10] Lin K, Zhang Y, Xu X, Di H, Yang R, Qin P. Modeling and simulation of underfloor electric heating system with shape-stabilized PCM plates. Building and Environment 2004;39:1427–34.
[11] Farid M., Chen W.J. (2001) Underfloor heating with latent heat storage. Proceedings of the Institution of Mechanical Engineers, Part A: Journal of Power and Energy 215(A5):pp. 601–609.
[12] Fallahi A, Haghighat F, El Sadi H. Energy performance assessment of double-skin facade with thermal mass. Building and Energy 2010;42:1499–509.
[13] Qiu K, Haghighat F. Modeling the combined conduction—air infiltration through building envelope. Building and Energy 2007;39:1140–50.
[14] Ibáñez M, Lázaro A, Zalba B, Cabeza LF. An approach to the simulation of PCMs in building applications using TRNSYS. Applied Thermal Engineering 2005;25:1796–807.
[15] Lamberg P., Jokisalo J., Sirén K. (2000). The effects on indoor comfort when using phase change materials with building concrete products. Proceedings of Healthy Buildings 2000, Vol. 2, pp. 751–756, SIY Indoor Air Information OY.
[16] Jokisalo J., Lamberg P., Sirén K. (2000). Thermal simulation of PCM structures with TRNSYS. Terrastock 2000, Stuttgart, Germany.
[17] Verma P, Singal SK. Review of mathematical modeling on Latent heat thermal energy storage systems using phase-change material. Renewable and Sustainable Energy Reviews 2008;12:999–1031.
[18] Swaminathan CR, Voller VR. On the enthalpy method. International Journal of Numerical Methods for Heat Fluid Flow 1993;3:233–44.
[19] Bonacina C, et al. Numerical solution of phase-change problems. International Journal of Heat and Mass Transfer 1973;16:1825–32.
[20] Cao Y, Faghri A. A numerical analysis of phase change problem including natural convection. Journal of Heat Transfer 1990;112:812–5.
[21] Gartling DK. Finite Element Analysis of Convective Heat Transfer Problems With Change of Phase. London, Pentech: Computer methods in fluids; 1980 pp 257–84.
[22] Haghighat F, Liang H. Determination of transient heat conduction through Building envelopes—a review. ASHRAE Transactions 1992;98:284–90.
[23] Haghighat F, Sander D, Liang H. An experimental procedure for deriving Z-Transfer functions coefficients of building envelope. ASHRAE Transactions 1991;97:90–8.
[24] Barbour JP, Hittle DC. Modeling phase change materials with conduction transfer functions for passive solar applications. Journal of Solar Energy Engineering 2006;128:58–69.
[25] Stupar, A., Drofenik, U., Kolar, J.W., (2010), Application of phase change materials for low duty cycle high peak load power supplies, CIPS, March, Nuremberg, Germany.
[26] Incropera FP, DeWitt DP, Bergman TL, Lavine AS. Fundamentals of Heat and Mass Transfer.5th Edition New York: Wiley; 2007.
[27] Johannes, K. and Virgone, J. (2011) TASK C Report of the Annex 23 of the International Energy Agency, Applying Energy Storage in Buildings of the Future, prepared, CETHIL Thermal center of Lyon School of Architecture.